Journal of Alloys and Compounds 536S (2012) S477–S479

Contents lists available at SciVerse ScienceDirect

Journal of Alloys and Compounds

journal homepage: www.elsevier.com/locate/jallcom

The role of pH and Mg on the stability and crystallization of amorphous calcium carbonate

J.D. Rodriguez-Blanco*, S. Shaw, P. Bots, T. Roncal-Herrero, L.G. Benning

School of Earth and Environment, University of Leeds, Leeds LS2 9JT, United Kingdom

ARTICLE INFO

Article history:
Received 23 June 2011
Received in revised form 24 October 2011
Accepted 11 November 2011
Available online 20 November 2011

Keywords:
Amorphous materials
Nanostructured materials
Crystal growth
Synchrotron radiation

ABSTRACT

The effects of pH and Mg on the crystallization of amorphous calcium carbonate (ACC) to vaterite and/or calcite were studied using a combination of *in situ* time resolved synchrotron-based techniques and electron microscopy. The experiments showed that Mg increased the stability of ACC and favoured the formation of calcite over vaterite. A neutral (~7) starting pH during mixing promoted the transformation of ACC into calcite via a dissolution/reprecipitation mechanism. Conversely, when ACC formed in a solution that started with a high initial pH (~11.5), the transformation to calcite occurred via metastable vaterite, which formed via a spherulitic growth mechanism. In a second stage this vaterite transformed to calcite via a surface-controlled dissolution and recrystallization mechanism. These crystallization pathways can be explained as a consequence of the pH-dependent composition, local structure, stability and dissolution rates of ACC.

1. Introduction

Amorphous calcium carbonate (ACC) is a hydrated, poorly ordered, nanoparticulate and metastable precursor to crystalline $CaCO_3$ (e.g., calcite, vaterite, aragonite). The crystallization of $CaCO_3$ polymorphs from ACC is a key process in the formation of many biominerals [1], which in turn control a large part of the global carbon cycle [2]. Furthermore, for many industrial applications (e.g., pharmaceuticals, dental care products, cleaning agents) [3] crystalline $CaCO_3$ compounds are often synthesized via an ACC precursor. It is well known that the formation, stabilization and crystallization of ACC are controlled by various factors including temperature, pH and dopants (e.g., Mg^{2+}, organics) [4–6]. For example, the crystallization rates and pathways of ACC to crystalline $CaCO_3$ as part of biomineralization processes in a variety of organisms are particularly affected by the content of Mg and pH. This results in the incorporation of variable amounts of Mg (generally from 4 to 15%) and different crystal morphologies [1–4]. However, the mechanisms of ACC formation and crystallization are poorly understood because the reactions can be rapid (e.g., in the pure system, seconds–minutes) and often proceed via intermediate phases [7]. These factors make time resolved characterizations of these reactions, using conventional off-line techniques, difficult. Recently however, with the capabilities of synchrotron-based techniques, *in situ* analysis of these complex reaction pathways has become possible [8,9]. In this study, we used *in situ* time-resolved synchrotron-based wide angle X-ray scattering (WAXS) and energy dispersive X-ray diffraction (ED-XRD), combined with off-line high resolution imaging to evaluate the effects of pH and Mg on the mechanism of ACC crystallization. We hypothesize that the pH of ACC formation and the presence of Mg^{2+} are the main parameters controlling the structure of the ACC and hence its stability, solubility and transformation pathway.

2. Experimental methods

ACC precipitation and crystallization experiments were carried out at 10–25 °C by rapidly mixing, under constant and vigorous stirring, equal volumes of 1 M Na_2CO_3 (pH = ~11.2) and $CaCl_2$ or $CaCl_2/MgCl_2$ (pH = ~6.7) solutions. In all cases immediately upon mixing ACC precipitated as a white gel. The effect of two mixing methods, thus two different initial pH's and of Mg as a dopant were tested as follows: (i) *experiment 1*, at 10 °C: pouring the high pH Na_2CO_3 solution into the neutral pH $CaCl_2$ solution; (ii) *experiment 2*, at 25 °C: pouring the low pH $CaCl_2$ solution into the high pH Na_2CO_3 solution; (iii) *experiment 3*, at 21 °C: pouring a neutral pH $CaCl_2/MgCl_2$ solution (Ca/Mg ratio = 9:1) into the high pH Na_2CO_3 solution. With *experiments 1 and 2* we explored the effect of initial pH on the crystallization of ACC in a pure system (non Mg-doped). As such, in *experiment 1*, the precipitation of ACC was initiated by adding the higher pH $NaCO_3$ solution to the lower pH $CaCl_2$, which caused the ACC to form while the pH of the mixed solution increased from 6.7 to ~11 (Fig. S1 in Supplementary Information). Conversely, in *experiment 2* the formation of ACC was initiated by adding the neutral pH $CaCl_2$ to the high pH $NaCO_3$ solution, which caused the ACC to form as the pH of the mixed solution decreased from pH ~11.2 to ~10.5 (Fig. S1). Finally, *experiment 3* was carried out the same way as *experiment 2* (i.e., high pH start), but with 10% of the Ca^{2+} replaced with Mg^{2+}. Once formed, ACC crystallized and the pH dropped further to reach an end value of ~8.0 (Fig. S1). The low (10 °C) temperature of *experiment 1* was selected to reduce the rate of crystallization and therefore maximize the acquisition of quantitative data in the on-line experiment.

The *in situ* ED-XRD experiments were performed on beamline 16.4 at the Daresbury Synchrotron Radiation Source, UK, and *in situ* WAXS experiments on beamline I22 at the Diamond Light Source Ltd. (UK). The experimental methodologies for the

* Corresponding author.
E-mail address: J.D.RodriguezBlanco@leeds.ac.uk (J.D. Rodriguez-Blanco).

0925-8388/$ – see front matter © 2011 Elsevier B.V. All rights reserved.
doi:10.1016/j.jallcom.2011.11.057

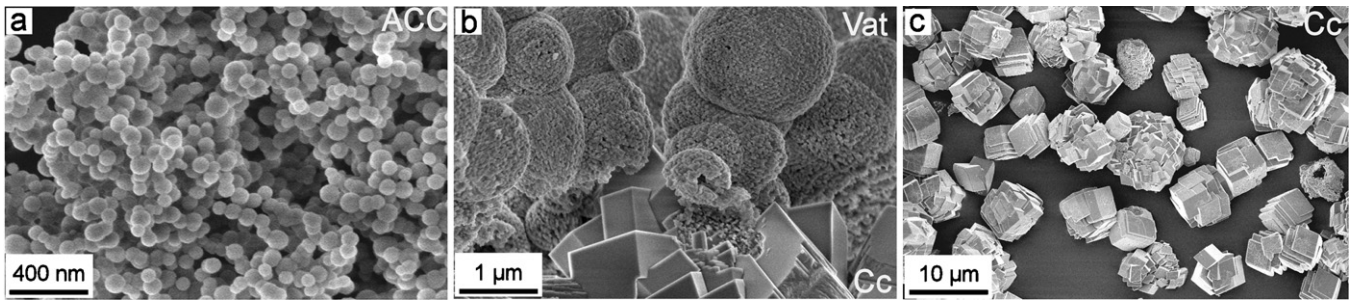

Fig. 1. Photomicrographs of (a) ACC nanoparticles formed immediately after mixing, (b) vaterite (Vat, spherical aggregates) and calcite (Cc, rhombohedra) observed after ~2 h and (c) end product calcite. Images show complete reaction in *experiment 2*.

ED-XRD and WAXS experiments, including data collection and processing, have previously been described in detail [8,9]. ED-XRD patterns were collected every minute with experiments lasting for up to 7 h, while WAXS patterns were collected every second and the experiment lasted ~1 h. Individual patterns were fitted using XFIT [10], and the areas of the Bragg peaks were normalized to values from 0 to 1 to express the degree of reactions (α) as a function of time. The change in background intensity (i.e., the intensity of a section of the WAXS or ED-XRD patterns with no peaks) with time was used to evaluate the amount of ACC present within each system [8].

Equivalent off-line experiments were used to (a) follow the evolution of the pH during the experiments and (b) produce samples for solid characterization. These off-line experiments, including pH measurements (Fig. S1), were repeated a minimum of three times to confirm reproducibility. Aliquots removed after specific times were filtered through 0.2 μm polycarbonate membranes and washed with water and isopropanol following Rodriguez-Blanco et al. [11]. Identification of solids was carried out by X-ray diffraction with a Bruker D8 X-ray Diffractometer (Cu $K\alpha_1$, range 10–60°, 0.001°/step and 0.1 s/step). Finally, the resulting solids were imaged with a field emission gun scanning electron microscope (FEG-SEM, LEO 1530 Gemini at 3 keV).

3. Results and discussion

In all experiments ACC formed instantaneously upon mixing. It consisted of ~50 nm spherical particles with low polydispersity and smooth surfaces (Fig. 1a). Off-line XRD scans of ACC (Fig. S2) showed no Bragg peaks but broad humps located at a 2θ of ~30° and ~45°, reflecting the poorly ordered nature of the solid. [11] In the first minutes (1–10 min) the ED-XRD and WAXS patterns showed only a broad hump in the background from the combined scattering of water and ACC. However, the subsequent evolution of the reactions varied dramatically depending on (a) the mixing sequence (i.e., starting pH) and (b) presence/absence of Mg.

In *experiment 1* (starting from a neutral pH; Fig. 2 and Fig. S1), the background intensity, and hence the amount of ACC, decreased rapidly with time and this was mirrored by the rapid growth of calcite. After ~10 min the background became stable (seemingly most ACC consumed), but the intensity of the calcite peak continued to slowly increase until ~35 min. The end product, calcite (Fig. S3), consisted of large rhombohedral crystals or crystal aggregates with numerous intergrowths (Fig. S5). The evolution of *experiment 2* (starting from high pH; Fig. 3 and Fig. S1) was different. The reaction was longer (hours) and ACC breakdown occurred in parallel with the initial formation of an intermediate, vaterite. This vaterite transformed to calcite in a second stage. The formation of vaterite was rapid (5–15 min) and the resulting crystals consisted of large spherical aggregates composed of <50 nm nanoparticles (Fig. 1b). Once vaterite was fully formed it slowly dissolved, while calcite crystals gradually grew on the surface of the vaterite nanoaggregates (Fig. 1b). The ED-XRD data (Fig. 3) revealed that vaterite decay and calcite growth mirrored each other during the transformation (~6 h). In *experiment 2*, the final product, calcite (Fig. 1c) was of similar size and morphology as those in *experiment 1* (Fig. S5). We observed the same pathway (vaterite decay and calcite growth) at a series of other temperatures with the same mixing approach [8]. Lastly, although the mixing procedure (i.e., high starting pH) in *experiment 3* (Fig. 2) and *experiment 2* (Fig. 3) were equivalent, the replacement of 10% of the initial Ca with Mg translated into a different reaction pathway compared to the pure system. In this case, ACC was stabilized for a longer time (~14 min) compared to both *experiments 1 and 2*. However, more importantly, calcite formed directly from ACC with no vaterite intermediate. The crystallization of ACC to calcite was fast; once initiated the reaction was completed in less than 10 min (Fig. 2; *experiment 3* and Fig. S4).

Experiments 1 and 2 revealed the importance of the initial mixing pH on the stability and crystallization pathway of ACC. The mixed Na_2CO_3 and $CaCl_2$ solutions naturally always reach the same mixed pH value (~10.5). However, the evolution of the pH during mixing

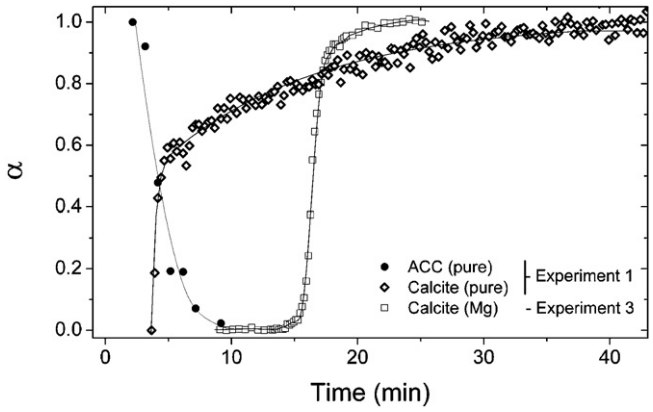

Fig. 2. Evolution of the degree of reaction (α) from WAXS data for pure ACC and calcite (*experiment 1*) and for calcite in the presence of 10% Mg (*experiment 3*). α's for calcite and ACC respectively were obtained from the (1 0 4) Bragg peak and from the background with no Bragg peaks. Lines are a guide to the eye.

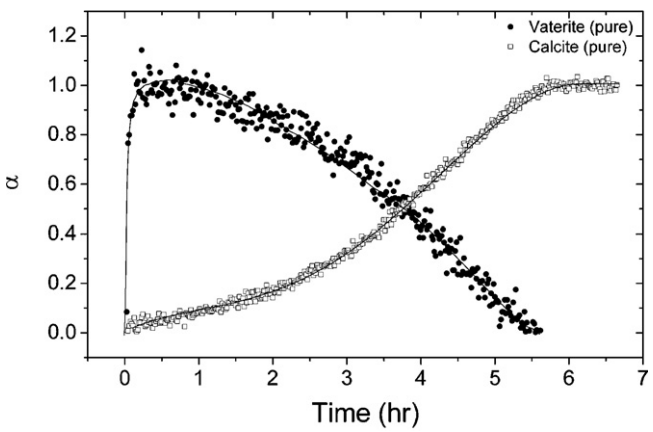

Fig. 3. Evolution of the degree of reaction (α) from ED-XRD data of the vaterite (1 0 1) and calcite (1 0 4) peaks as a function of time for *experiment 2*. Lines are a guide to the eye only.

had a critical effect on the crystallization pathways. When mixing started from a neutral pH (i.e., *experiment 1*, Fig. 2 and Fig. S1) the initial ACC transformed directly to calcite (Figs. S3 and S5). Conversely when mixing started from a high pH (*experiment 2*, Fig. 3) vaterite formation was triggered and the system was driven through a much slower, two stage reaction to calcite. The local structure of ACC has been shown to be a function of the synthesis pH, which is linked to the aqueous speciation of carbonate during ACC formation [12,13]. Gebauer et al. [13] suggested that the short-range structure of ACC depends on the binding strength of Ca^{2+} and CO_3^{2-} ions within the ACC precursor clusters. They asserted that this binding strength is inversely related to pH and this is key in controlling the structure and stability of ACC: at neutral- or high-pH, ACC exhibits a local structure similar to calcite or vaterite, respectively. Based on our data, we argue that this pH-dependent local structure of the precursor ACC controls the crystallization pathway. Mixing from a neutral pH (*experiment 1*) produces ACC with a calcite local structure that will crystallize directly to calcite, while mixed from a high pH (*experiment 2*) forms ACC with a vaterite local structure, thus calcite formation will proceed through the vaterite intermediate. Other experimental studies [12,13] have shown that the solubility and dissolution rate of ACC at neutral to alkaline pH (7–10) increases proportionally to the pH at which it is formed. Therefore, the solution in equilibrium with ACC formed at a high pH, would have a higher supersaturation with respect to $CaCO_3$ compared to that of ACC formed at neutral pH. High supersaturation levels are needed for the nucleation of vaterite (see below). Thus the formation of a high-pH ACC precursor favours vaterite formation over calcite, and calcite only forms in a secondary stage.

Both the ED-XRD and WAXS data clearly demonstrated that ACC breaks down to either vaterite or calcite in all experiments. ACC is a highly hydrated compound [11,14] so its breakdown may involve a dehydration process [8]. The fast ACC breakdown prior to vaterite formation supports a rapid increase in supersaturation, combined with the spherical morphology of the vaterite particles formed indicates a spherulitic growth mechanism [15]. This supports Andreassen et al. [16], who suggested that ACC transforms to vaterite via a spherulitic growth mechanism following a growth front nucleation process [17]. Both our current on-line and off-line data support this mechanism [15]. The formation of calcite in stage 2 of *experiment 2* leads to a gradual increase in porosity of the vaterite spherulites due to its dissolution and transformation to calcite [8] (Fig. 1b). This occurs slower than stage 1 and via a surface controlled dissolution–reprecipitation process [8]. In this experiment it was particularly clear how the change in the degree of reaction with time for vaterite (breakdown) and calcite (growth) mirrored each other, proceeding faster as the surface area of calcite increased. This interpretation is in agreement with Ogino et al. [18], who studied the vaterite–calcite transformation in seeded systems and Rodriguez-Blanco et al. [8], who evaluated the rates and energetics for this reaction as a function of temperature.

Finally, as seen in *experiment 3*, Mg had a noteworthy effect on both the stability of ACC and its transformation to crystalline $CaCO_3$ (Fig. 2 and Fig. S4). In the pure system the formation of crystalline $CaCO_3$ started between <1 and 4 min (10–25 °C) [7]. In the presence of Mg at 21 °C the induction time was 14 min (Fig. 2). This suggests that regardless of temperature, Mg greatly increased the induction time for $CaCO_3$ crystallization, which compared with the pure system is one order of magnitude longer and no vaterite formed (Fig. 2; *experiment 3*). The only stable $CaCO_3$ polymorph, calcite, fully crystallized in less than 30 min. The effect of Mg in stabilizing ACC and its role in crystallization has been recently [6,19,20] attributed to the high dehydration energy of the Mg ion. [21] Mg present within the porous structure of ACC is likely to retard its dehydration, therefore reducing the rate of dissolution and potentially decreasing its overall solubility. This reduction in solubility lowers the supersaturation level within the solution. This would favour the surface-controlled growth mechanism of calcite, and limit the nucleation dominated pathway of vaterite crystallization. Furthermore, this direct transformation of ACC into calcite can be also a consequence of the instability of the vaterite structure at high Mg concentrations [6].

4. Conclusions

Our experiments showed that pH and Mg have a significant effect on the pathways and mechanisms of the transformation of ACC into crystalline $CaCO_3$. A neutral starting pH or the presence of Mg in solution drives the system towards a direct crystallization of ACC to calcite. Conversely, a high starting pH promotes the formation of the metastable intermediate, vaterite, driving the system towards calcite through a secondary dissolution–recrystallization step. Mg increases the stability of ACC and inhibits vaterite crystallization, favouring the direct transformation of ACC to calcite. These mechanisms and pathways have significant implications for industrial carbonate formation, for processes linked to CO_2 capture and storage as well as biomineralization and thus the global carbon cycle.

Acknowledgements

This study was supported by the Marie Curie EU-FP6 Mineral Nucleation and Growth Kinetics (MIN-GRO) Research and Training Network under contract MRTNCT-2006-035488. The synchrotron work was funded via beam time access grants by CCLRC (grant nos: 50115 and 50218, Daresbury Laboratory), and Diamond Light Source (grant nos: SM4595 and SM1132) to Liane G. Benning. The insightful comments of anonymous reviewers are also gratefully acknowledged.

Appendix A. Supplementary data

Supplementary data associated with this article can be found, in the online version, at doi:10.1016/j.jallcom.2011.11.057.

References

[1] M. Faatz, F. Grohn, G. Wegner, Mater. Sci. Eng. 25 (2005) 153–159.
[2] R. Reeder, Rev. Mineral. 11 (1983) 1–47.
[3] F.W. Tegethoff, Calcium Carbonate, 1st edition, Birkhäuser, Basel, 2002.
[4] R.A. Berner, Geochim. Cosmochim. Acta 39 (1975) 489–494.
[5] Z. Chen, Z. Nan, J. Colloid Interface Sci. 358 (2011) 416–422.
[6] P. Bots, L.G. Benning, R.E.M. Rickaby, S. Shaw, Geology 39 (2011) 331–334.
[7] T. Ogino, T. Suzuki, K. Sawada, Geochim. Cosmochim. Acta 51 (1987) 2757–2767.
[8] J.D. Rodriguez-Blanco, S. Shaw, L.G. Benning, Nanoscale 3 (2011) 265–271.
[9] I. Ahmed, L.G. Benning, G. Kakonyi, A. Sumoondur, N. Terrill, S. Shaw, Langmuir 26 (2010) 6593–6603.
[10] R.W. Cheary, A. Coelho, J. Appl. Crystallogr. 25 (1992) 109–121.
[11] J.D. Rodriguez-Blanco, S. Shaw, L.G. Benning, Mineral. Mag. 72 (2008) 283–286.
[12] Y. Kojima, A. Kawanobe, T. Yasue, Y. Arai, J. Ceram. Soc. Jpn. 101 (1993) 1145–1152.
[13] D. Gebauer, A. Volkel, H. Colfen, Science 322 (2008) 1819–1822.
[14] A.L. Goodwin, F.M. Michel, B.L. Philips, D.A. Keen, M.T. Dove, R. Reeder, Chem. Mater. 22 (2010) 3197–3205.
[15] P. Bots, J.D. Rodriguez-Blanco, T. Roncal-Herrero, S. Shaw, L.G. Benning, Mineral. Mag. 75 (2011) 559.
[16] J.P. Andreassen, E.M. Flaten, R. Beck, A.E. Lewis, Chem. Eng. Res. Des. 88 (2010) 1163–1168.
[17] L. Gránásy, T. Pusztai, G. Tegze, J.A. Warren, J.F. Douglas, Phys. Rev. E 72 (2005) 011605.
[18] T. Ogino, T. Suzuki, K. Sawada, J. Cryst. Growth 100 (1990) 159–167.
[19] J. Jiang, M.R. Gao, Y.H. Qiu, S.H. Yu, Nanoscale 2 (2010) 2358–2361.
[20] Y. Politi, D.R. Batchelor, P. Zaslansky, B.F. Chmelka, J.C. Weaver, I. Sagi, S. Weiner, L. Addadi, Chem. Mater. 22 (2010) 161–166.
[21] D. di Tommaso, N. de Leeuw, Phys. Chem. Chem. Phys. 12 (2010) 894–901.